First Results from MoNA

A. Schiller[*], T. Baumann[*], D. Bazin[*], J. Brown[†], P. DeYoung[*,**], N. Frank[*,‡], A. Gade[*], J. Hinnefeld[§], R. Howes[¶], R. A. Kryger[‖], J.-L. Lecouey[*], B. Luther[††], W. A. Peters[*,‡], J. R. Terry[*,‡], M. Thoennessen[*,‡] and K. Yoneda[*]

[*]*National Superconducting Cyclotron Laboratory, Michigan State University, East Lansing, MI 48824*
[†]*Department of Physics, Wabash College, Crawfordsville, IN 47933*
[**]*Department of Physics & Engineering, Hope College, Holland, MI 49423*
[‡]*Department of Physics & Astronomy, Michigan State University, East Lansing, MI 48824*
[§]*Department of Physics & Astronomy, Indiana University at South Bend, South Bend, IN 46634*
[¶]*Department of Physics, Marquette University, Milwaukee, WI 53201*
[‖]*Molecular Separation Specialists LLLP, Lakeland, FL 33815*
[††]*Department of Physics, Concordia College, Moorehead, MN 56562*

Abstract. We explore the limits of nuclear stability and the consequences on nuclear structure theory by measuring masses of neutron-unbound nuclei and level energies above the neutron separation energy such as for the first excited state in ^{24}O. Open problems in reaction theory are addressed by, among others, measurements of the Coulomb breakup of ^{8}Li on a Pb and C target at 40 and 70 MeV/u.

Keywords: neutron-fragment coincidences, ^{24}O first excited level, ^{8}Li breakup on Pb and C at 40 and 70 MeV/u
PACS: 21.10.Dr, 23.90.+w, 25.60.Gc, 29.30.Hs

INTRODUCTION

Nuclei far from stability continue to be an exciting field of research. From a nuclear-structure point of view, two of the most interesting features are (i) the emergence of new magic numbers which come about by a re-ordering of single-particle levels for large proton-neutron asymmetries [1, 2] and (ii) the existence of very lightly bound nuclei with small particle-separation energies. Such systems, in the absence of significant Coulomb and angular-momentum barriers are quite loosely confined and often exhibit large exponential tails in their wavefunctions producing a halo [3].

Progress in radioactive beam research comes hand in hand with improvements in the understanding of nuclear reactions. The production of rare isotopes in fragmentation reactions is one of the most fundamental problems in the research area of fast radioactive beams [4]. As spectroscopic tools, knockout reactions have become one of the staples in the field [3]. Spectroscopic factors which lie at the interface of reaction theory and nuclear structure are now again, just as 40 years ago, the defining quantities for mapping out the nuclear shell structure [5]. Complementary to direct reactions are reactions via Coulomb excitation [6] or Coulomb breakup [7]. The former (sometimes supplemented by inelastic proton scattering in inverse kinematics [8]) is mostly concerned with low-energy (quadrupole) collectivity and the magnitude of low-lying $E2$ strength, the latter

CP831, *Frontiers in Nuclear Structure, Astrophysics, and Reactions: FINUSTAR*
edited by S. V. Harissopulos, P. Demetriou, and R. Julin

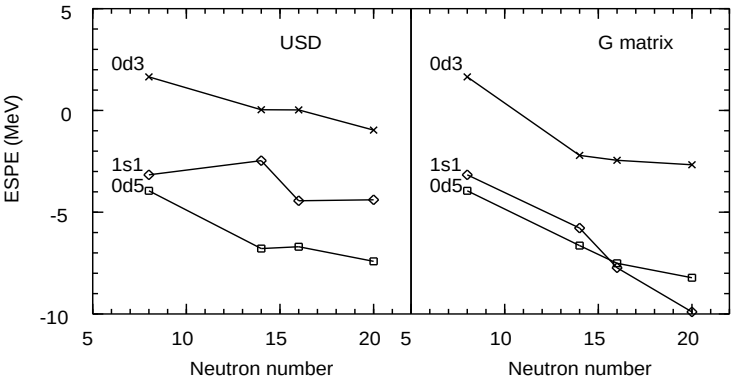

FIGURE 1. Effective single-particle energies in oxygen isotopes as a function of neutron number. Right panel: using a Brueckner *G*-matrix scheme to extract an effective interaction from nucleon-scattering data [9]. Left panel: using a phenomenological fit of the two-body interaction to nuclear structure data in the *sd* shell, the modified USD interaction. The figure is courtesy of B. A. Brown.

probes more the electric dipole strength, especially at higher beam energies [10]. Cross-sections of Coulomb-breakup reactions have also been used to obtain spectroscopic factors [11, 12].

THEORETICAL CONSIDERATIONS

We will concentrate our discussions on a few aspects of nuclear structure far from stability such as the emergence of new magic numbers. For this, a useful quantity to consider is the effective single-particle energy which is the sum of the single-particle energy and some diagonal two-body matrix elements. When the gap between completely filled and empty single-particle levels is large, two-body interactions such as the pairing force or the quadrupole-quadrupole force cannot induce significant correlations and the nuclear spectrum will exhibit a rather large first excited state energy. At the other extreme, when shells are half filled and single-particle levels are nearly degenerate, residual interactions can induce pairing correlations and large quadrupole collectivity [13]. The corresponding spectra will often exhibit low-lying excitations which can be populated via large transition matrix elements from the ground state.

In the case of the heavy oxygen isotopes, Fig. 1 shows the evolution of the neutron effective single-particle energies with neutron number. Since the effective single-particle energies contain contributions from diagonal two-body matrix elements, they will depend on occupation numbers. The results from a Brueckner *G*-matrix renormalization scheme shows a rather smooth dependence of the effective single-particle energies on neutron number. The $1s_{1/2}$ and $0d_{5/2}$ levels remain almost degenerate with a large gap to the $0d_{3/2}$ level, which is actually a resonance state in ^{17}O. The figure for the USD in-

teraction shows a gap evolving between the $1s_{1/2}$ level and the $0d_{5/2}$ level which attains its maximum width for ^{22}O, i.e., where the $0d_{5/2}$ subshell is completely filled while the $1s_{1/2}$ and $0d_{3/2}$ subshells are empty. Thus, the modified USD interaction (in contrast to the interaction based on the *G*-matrix) predicts ^{22}O to be a magic nucleus. Moreover, this gap diminishes rapidly when two more neutrons are added to the system. Instead, a new gap develops between the now filled $1s_{1/2}$ and $0d_{3/2}$ levels, making ^{24}O a magic nucleus as well. These considerations have been reported in [1, 2]. The differences between the USD and *G*-matrix predictions stem mostly from differences in their monopole terms. To our knowledge, it is not clear today what causes this monopole migration. Possible candidates are alterations of the interaction matrix elements associated with the $\sigma \cdot \tau$ operator with increasing proton-neutron asymmetry or the presence of true three-body interactions.

Similar effects are discussed for heavier nuclei up to Ca [14] and lighter *p*-shell nuclei. Neutron-rich *p*-shell nuclei exhibit inversion of the shell structure where the neutron $1s_{1/2}$ orbital becomes lower than the $0p_{1/2}$ orbital resulting in a $1/2^+$ ground state of ^{11}Be and large admixtures of $1s^2_{1/2}$ and $0d^2_{5/2}$ components in the ground-state wave function of ^{12}Be.

Such changes in the shell structure have implications for nuclear observables. The proposed magicity of ^{24}O can, e.g., be tested directly by measuring the excitation energy of its first excited state (it has been shown to be unbound against neutron emission [15]). Preliminary results for ^{24}O are presented here. Other projects of the MoNA collaboration exploring the shell structure of neutron-rich nuclei include: (i) an experiment on the decay energy of the neutron-unbound ground state of ^{25}O into the ground state of ^{24}O which is an indirect measure of the effective single-particle energy of the $0d_{5/2}$ orbital; (ii) an experiment on the cross section of the neutron-knockout reaction populating the $0d_{5/2}$ resonance in ^{11}Be which gives a direct measure of the $0d^2_{5/2}$ component of the ground-state wavefunction of ^{12}Be; and (iii) an experiment on the decay energies of the neutron-unbound ^{12}Li and ^{13}Li into ^{11}Li and one or two neutrons, respectively, which constrains the evolution of the effective single-particle energies for extreme ratios of neutrons and protons in the important transition region between the *p* and *sd* shell.

EXPERIMENTAL DETAILS

Fast radioactive beams are produced by the method of in-flight fragmentation [4] (see Fig. 2). A primary, stable beam is accelerated by the Coupled-Cyclotron Facility of the National Superconducting Cyclotron Laboratory to beam energies of typically 100–150 MeV/u. The coupling of two cyclotrons makes it possible to pre-accelerate ions at a low charge state with the K500 Cyclotron with more intensity and then create higher charge states by means of a stripping foil before further acceleration in the K-1200 Cyclotron.

Rare isotopes are produced by in-flight fragmentation at the production target. This target is typically a Be target, the thickness of which can be optimized to maximize the yield of a desired fragment at the focal plane of the A1900 fragment separator [16]. A thick production target increases on the one hand the number of produced isotopes, on

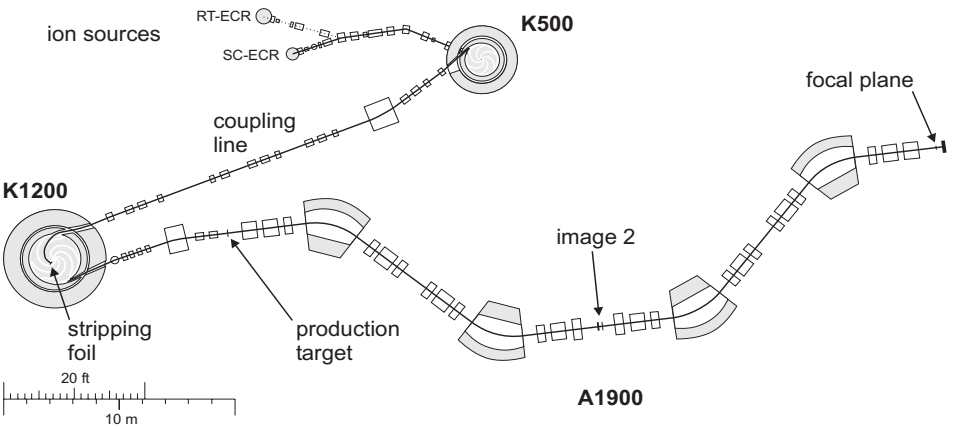

FIGURE 2. Production mechanism of fast radioactive beams. The main components are: an ion source to produce ions out of stable isotopes, the K500 Cyclotron for pre-acceleration, a stripping foil for creating highly charged ions, the K1200 Cyclotron main accelerator, the production target for radioactive isotopes and the A1900 fragment separator which selects rare beams based on their magnetic rigidity and energy-loss properties in a wedge at the image-2.

the other hand, it broadens their momentum distribution. Since the A1900 is basically a momentum filter, one has to balance these two consideration to achieve a maximum yield.

Different isotopes are produced with different momentum distributions. The fields of the first two dipoles of the A1900 are set corresponding to the maximum of the momentum distribution of the desired fragment. This removes undesired fragments which exhibit significantly different momentum distributions. To further clean up the beam, a wedge-shaped degrader is introduced at the image-2 plane of the A1900. Different isotopes (but with, at this point, about equal magnetic rigidity) will experience different degrees of energy loss. This will, in consequence, shift the maxima of their momentum distributions in different ways. The thickness of the wedge can again be optimized, where a thick wedge improves isotopic separation while it also broadens the momentum distribution of the desired fragment and hence reduces its final yield. The fields of the last two dipoles are again set corresponding to the maximum of the now shifted momentum distribution of the desired fragment. Typical fragment-beam energies are in the order of 70 MeV/u. The beam purity can be determined by the ΔE-ToF technique at the focal plane. In favorable cases, the fragment beam can be almost 100% pure. In most other cases, undesired fragments will distinguish themselves by a significantly different ToF from the focal plane of the A1900 to the secondary reaction target at the experiment. By means of fast scintillators at those two positions, beam particles can be identified isotopically in the offline analysis event by event.

The experimental setup (see Fig. 3) consists of tracking detectors for the incoming beam which are used to determine the angle and more importantly the position of the beam particles on the secondary reaction target. At 8–14 m behind the reaction target,

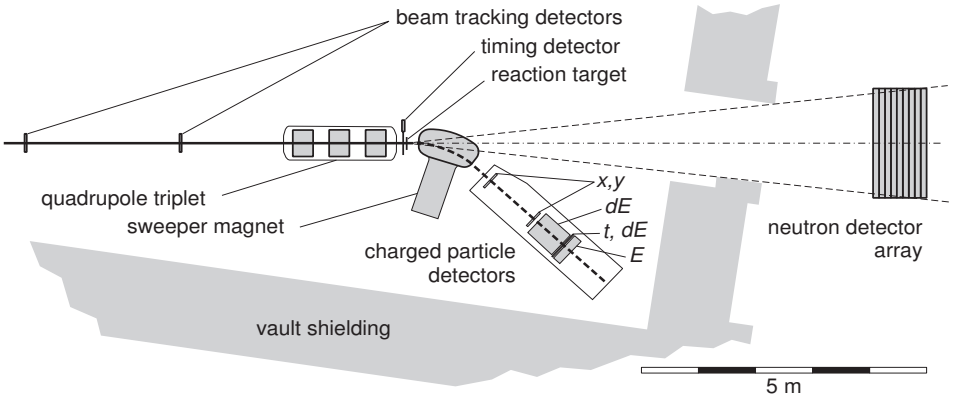

FIGURE 3. Experimental setup. The incoming beam is tracked in position and angle and identified event by event using tracking and timing detectors, respectively. The timing detector serves also as start for the fragment and neutron ToF. A diamond detector has been tested at this spot for high-rate applications. Behind the secondary reaction target neutrons are detected around 0° with MoNA; charged fragments are detected by a suite of two CRDCs (x,y), an ion chamber (dE), a thin (t,dE), and a thick (E) scintillator behind a wide-gap sweeper magnet which bends the desired products into roughly 40°.

neutrons are detected by the modular neutron array (MoNA) [17]. It consists of 9×16 horizontal plastic-scintillator bars of 2 m length each with photomultipliers mounted on both ends. This gives a position resolution on the order of a $\sim$10 cm in each direction. Discrimination against γ rays is performed by the ToF method. Charged particles are bent into 43° by a wide-gap sweeper magnet [18]. The atomic number is determined from energy-loss spectra in an ion chamber. Isotopic identification is performed by ToF spectra which are corrected for target position, position on the timing detector, and position and angle behind the magnet. Angle and energy at the target position are determined by a reconstruction of the flightpath through the magnet. This becomes an overdetermined problem once the position of the incoming beam has been measured by means of the beam tracking detectors. The thickness of the reaction target can be chosen to maximize the yield as long as isotopic resolution of the products is not compromised.

Coincident recording of energy-momentum vectors of neutrons and charged fragments allows us to reconstruct the invariant mass of the decaying state which can be translated into decay energy with the help of the known masses of the particle-bound decay products. With the present setup we have achieved isotopic separation of charged fragments up to oxygen isotopes. On the other hand, some detectors, most notably the ion chamber, the beam-tracking detectors, and the CRDCs become inefficient for He and H isotopes. The expected resolution of the invariant mass spectrum is in the order of $\sim$ 300 keV but depends to some degree on target thickness. The combination of high beam energy and large geometric acceptance of MoNA allows us to determine decay energies reliably up to $\sim$ 1 MeV. In the case of reaction products with rather similar magnetic rigidities as the rare-isotope beam (as in the case of neutron knockout or Coulomb breakup), a beam blocker has to be introduced in front of the charged-particle

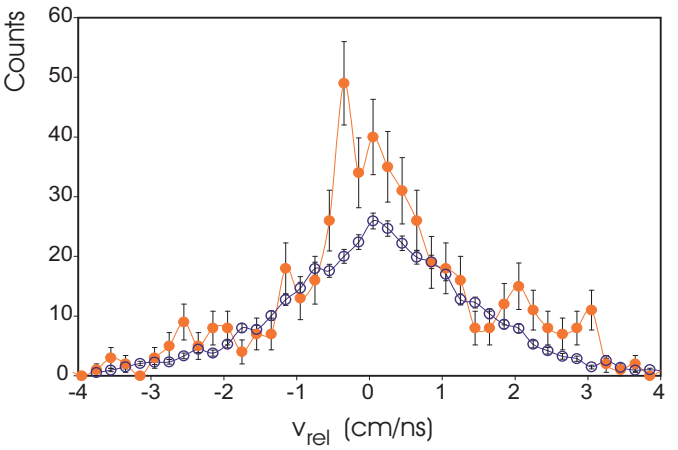

FIGURE 4. Difference spectrum between ^{23}O and neutron velocity. Upper line, full symbols: experimental spectrum, lower line, open symbols: experimental estimate of coincident neutrons not related to excitations in ^{24}O. The velocity difference at which the two curves depart can directly be related to a decay energy of around ~ 0.3 MeV. A significantly larger decay energy of 1 MeV or higher would create a dip in the spectrum around zero due to the finite geometric acceptance of MoNA. This is not supported by our data, thus an excitation energy of the first excited state in ^{24}O above the suggested 4.8 MeV from Ref. [19] can most likely be excluded.

detectors in order to limit the rate to the maximum of ~ 200 triggers per second. Such a beam blocker introduces additional acceptance cuts. To investigate the effects of our geometric acceptance cuts for neutrons and fragments on invariant-mass spectra, we have performed a measurement of the previously known Coulomb-breakup reaction of ^{11}Be and the decay of ^{7}He produced by proton knockout from a ^{8}Li beam.

PRELIMINARY RESULTS

Our first study concerned the energy of the first excited state of ^{24}O populated by two-proton knockout. A preliminary velocity-difference spectrum from the latter experiment (i.e., a simpler substitute for a decay-energy spectrum, see Fig. 4) indicates a decay-energy of around ~ 0.3 MeV translating into an excitation energy for the first excited state of ~ 3.9 MeV which is about 0.9 MeV less than in a recent calculation using the modified USD interaction [19]. This result might suggest that ^{24}O is somewhat less magic than expected, however, simulations indicate that our systematic uncertainties at this point are too high to firmly rule out the calculations of Ref. [19].

An open question in Coulomb breakup is the presence of two widely different predictions of the Coulomb-breakup cross section of a *p*-wave neutron such as in ^{8}Li. While CDCC calculations favor small decay energies of ~ 0.51 MeV and produce larger cross sections, the adiabatic model tends to favor larger decay energies of ~ 1.5 MeV and smaller cross sections by more than a factor of two. Such differences in model predic-

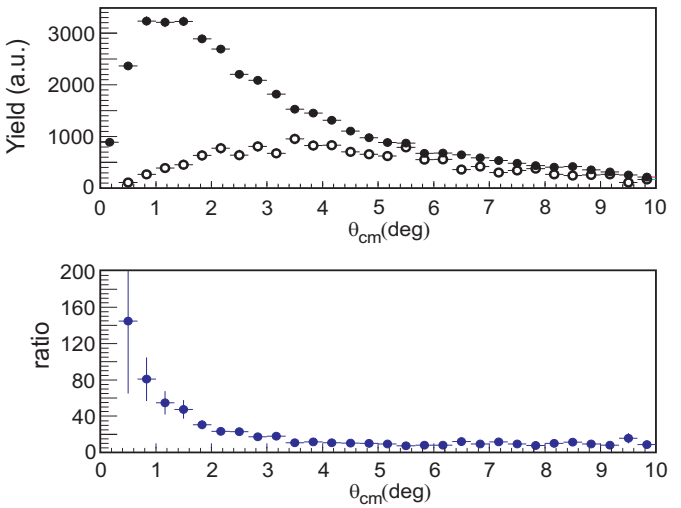

FIGURE 5. Upper panel: coincident fragment-neutron yield as function of opening angle in the CM system for 40 MeV/u ^{8}Li on Pb (solid symbols) and on C (open symbols). Lower panel: ratio of the two yields. Figure taken from [20].

tions are much less pronounced for the breakup of an *s*-wave neutron state such as for the breakup of ^{11}Be where good data already exist. Preliminary results [20] from our Hungarian and Japanese collaborators show coincidence yields as function of opening angle for a Pb and C target (see Fig. 5). The differences are marked and we expect that we can separate the nuclear- from the Coulomb-breakup component in the reaction of ^{8}Li on Pb.

CONCLUSION AND OUTLOOK

We have started an exciting experimental research program on the consequences of the evolution of effective single-particle levels far from stability on nuclear-physics observables. Preliminary results on the excitation energy of the first excited state in ^{24}O have been discussed. These results show that ^{24}O might be somewhat less magic than recent model predictions suggest. This project is complemented by a variety of experiments which we can only mention here. E.g., we have performed an experiment on the decay energy of ^{25}O and on the neutron-knockout reaction cross section of ^{12}Be into the neutron-unbound $0d_{5/2}$ state of ^{11}Be. Our decay energy spectrum for the latter experiment is in good agreement with a similar work at GANIL [21]. The complication with this experiment is the presence of coincident neutrons from possible dissociation of ^{12}Be. Our large efficiency compared to the Demon array used for the GANIL experiment might help both groups to elucidate the contribution of these dissociation neutrons to the decay-energy spectrum. Furthermore, an experiment on the production and decay of ^{12,13}Li has been tentatively scheduled.

Our work on nuclear reactions has mostly focused on investigations of the Coulomb breakup of ^{8}Li for which different model predictions exists. Concerning fragment production, we have performed an experiment on the fragmentation of a 140 MeV/u ^{48}Ca beam where we observed neutrons in coincidence with fragments in order to better understand the later stages of the production of rare isotopes in fragmentation.

Data analysis for all of our projects is progressing and more experiments are scheduled or are in a planning stage. We hope to be able to present more final results in the near future for the projects mentioned in this work.

ACKNOWLEDGMENTS

We would like to thank the other members of the MoNA collaboration: J. Finck, C. Hofman, K. Jones, K. Kemper, P. Pancella, G. Peaslee, W. Rogers, S. Tabor, and about 50 undergraduate students for their contributions to this work. We would also like to thank B. A. Brown for the Fig. 1, and C. Bordeanu, N. Carlin, M. Csanád, F. Deák, T. Fukuchi, Zs. Fülöp, D. R. Galaviz, A. Galonsky, Á. Horváth, K. Ieki, R. Izsák, Á. Kiss, H. Schelin, Z. Seres, R. Sugo, and G. Veres for letting us present their data on the ^{8}Li Coulomb-breakup reaction. Financial support from the National Science Foundation under grant numbers PHY-01-10253 and PHY-03-54920 is gratefully acknowledged.

REFERENCES

1. T. Otsuka, R. Fujimoto et al., *Phys. Rev. Lett.* **87**, 082502 (2001).
2. Y. Utsuno, T. Otsuka et al., *Phys. Rev. C* **64**, 011301(R) (2001).
3. P. G. Hansen and B. M. Sherrill, *Nucl. Phys.* **A693**, 133–168 (2001).
4. G. D. Westfall, T. J. M. Symons et al., *Phys. Rev. Lett.* **43**, 1859–1862 (1979).
5. A. Gade, D. Bazin et al., *Phys. Rev. Lett.* **93**, 042501 (2004).
6. T. Glasmacher, *Nucl. Phys.* **A693**, 90-104 (2001).
7. N. Fukuda, T. Nakamura et al., *Phys. Rev. C* **70**, 054606 (2004).
8. H. J. Ong, N. Imai et al., *Eur. Phys. J. A* **25**, 347–348 (2005).
9. M. Hjorth-Jensen, T. T. S. Kuo, and E. Osnes, *Phys. Rep.* **261** 125–270 (1995).
10. P. Adrich, A. Klimkiewicz et al., *Phys. Rev. Lett.* **95**, 132501 (2005).
11. T. Nakamura, S. Shimoura et al., *Phys. Lett. B* **331**, 296–301 (1994).
12. R. Palit, P. Adrich et al., *Phys. Rev. C* **68**, 034318 (2003).
13. D. J. Dean and M. Hjorth-Jensen, *Rev. Mod. Phys.* **75**, 607–656 (2003).
14. E. Caurier, G. Martinez-Pinedo et al., *Rev. Mod. Phys.* **77**. 427–488 (2005).
15. M. Stanoiu, F. Azaiez et al., *Phys. Rev. C* **69**. 034312 (2004).
16. D. J. Morrissey, B. M. Sherrill et al., *Nucl. Intrum. Methods Phys. Res.* **B204**, 90–96 (2003).
17. T. Baumann, J. Boike et al., *Nucl. Instrum. Methods Phys. Res.* **A543**, 517–527 (2005).
18. M. D. Bird, S. J. Kenney et al., *IEEE Trans. Appl. Supercond.* **15**, 1252–1254 (2005).
19. A. Volya and V. Zelevinsky, *Phys. Rev. Lett.* **94**. 052501 (2005).
20. Á. Horváth, K. Ieki et al., *Eur. Phys. J. A* (to be published).
21. S. D. Pain, W. N. Catford et al., *Eur. Phys. J. A* **25**, s01, 349–351 (2005).